The International Journal of Advanced Manufacturing Technology (2022) 120:7565–7574
https://doi.org/10.1007/s00170-022-09117-z

ORIGINAL ARTICLE

Machinability investigations in cryogenic internal cooling turning Ti-6Al-2Zr-1Mo-1 V titanium alloy

Yongquan Gan[1] · Yongqing Wang[1] · Kuo Liu[1] · Yuebing Yang[1] · Shaowei Jiang[1] · Yu Zhang[1]

Received: 22 December 2021 / Accepted: 24 March 2022 / Published online: 29 April 2022

Abstract

Because of its outstanding strength-to-density ratios, corrosion resistance, and other superior properties, Ti-6Al-2Zr-1Mo-1 V titanium alloy (TA15) is widely employed in aeronautics and astronautics. TA15 is a typical difficult-to-cut material with low heat conductivity, a high cutting temperature, and an easy adhesion characteristic. When machining difficult-to-cut materials, cryogenic machining is an efficient way to lower the cutting temperature. There is, however, few research on machining TA15 under cryogenic cooling conditions. In this study, tensile tests were performed under different low-temperature cooling conditions. By analyzing the changes of material properties under different low temperatures, the machining mechanism of TA15 under cryogenic cooling conditions was revealed. Then, cutting experiments were carried out under three cooling conditions: dry, cutting fluid (wet), and liquid nitrogen internal cooling (cryogenic). The results show that under cryogenic conditions, TA15 can effectively reduce plasticity and adhesion. The cutting experiments also prove that machining TA15 under the cryogenic cooling condition can reduce the surface adhesion, improve the machining quality of the machined surface, and effectively reduce the generation of tool adhesion wear.

Keywords Cryogenic internal cooling · Ti-6Al-2Zr-1Mo-1 V titanium alloy (TA15) · Material properties · Surface integrity · Tool wear

1 Introduction

At present, titanium alloys are finding wide application in aeronautics, astronautics, biomedical, and so on because of the excellent strength to density ratios and corrosion resistance [1, 2]. However, titanium alloys generally have the characteristics of poor thermal conductivity and high cutting temperature [3]. Therefore, when cutting titanium alloys, a large quantity of heat will be generated, which leads to poor surface quality and serious tool wear and other machining defects [4, 5]. Many scholars have explored the machining of titanium alloys. Among them, cryogenic machining was a method of applying cooling to the cutting area using a cryogenic medium, aiming to reducing the temperature, increase the tool life and improve the surface integrity [6, 7]. Liquid nitrogen (LN_2, −196 °C) is one of the most commonly used cooling media in cryogenic machining [8, 9]. Nitrogen is a colorless, tasteless, non-toxic, and harmless inert gas; 79% of the air is composed of nitrogen [10]. Using liquid nitrogen as the cryogenic cooling mediums in machining can not only effectively reduce cutting temperature, but also realize the safety and environmental protection, and reduce the difficulty of cleaning treatment. After liquid nitrogen evaporates, it will return to the atmosphere without any pollution.

In terms of the effect of liquid nitrogen cooling machining, many scholars have made some research on different kinds of materials, such as AISI 52,100 harden steel [11], Co–Cr–Mo alloys [12], magnesium alloys [13], porous tungsten [14], CFRP [15], and PTFE [16]. It achieved outstanding machining performance in the aspects of surface integrity or tool wear and so on in the cryogenic machining of the above materials.

At present, in the research of cryogenic machining of titanium alloy, scholars have mainly carried out relevant research on Ti-6Al-4 V (TC4) titanium alloy [17–19]. However, few scholars have carried out relevant research on cryogenic machining of Ti-6Al-2Zr-1Mo-1 V titanium alloy (TA15). Different from the microstructure of α + β phase in

✉ Kuo Liu
liukuo@dlut.edu.cn

[1] Key Laboratory for Precision and Non-Traditional Machining Technology of Ministry of Education, Dalian University of Technology, Dalian 116024, China

Table 1 Chemical composition of TA15 alloy (mass fraction, %)

Al	N	H	Fe	C	Mo	V	Ti
6.55	0.009	0.01	0.2	0.08	0.94	0.82	Bal

TC4 titanium alloy, TA15 titanium alloy is a near-α titanium alloy, which is widely used as the key load-bearing structural part in some extreme conditions, as well as the compressor blades and compressor disks of gas turbine engines [1, 20]. Compared with the α + β phase, the α phase has better ductility and is more prone to adhesion [21]. Due to the different microstructures, cryogenic machining performance is bound to be different.

In this paper, the applicability of TA15 titanium alloy cryogenic internal machining is studied. The mechanical properties of TA15 titanium alloy with temperature change were studied through tensile tests at different temperatures, and the mechanism of material properties with temperature change was analyzed, which provides a theoretical basis for cryogenic machining TA15. Then, the effectiveness of cryogenic internal turning of TA15 was studied by comparing the machined surface morphology, machined surface roughness, and tool wear under three cooling conditions: dry, cutting fluid (wet), and liquid nitrogen internal cooling (cryogenic). The research of this paper provides a theoretical and experimental basis for cryogenic machining of TA15.

2 Experimental

There are two parts to the experiments. In order to analyze the change of material property under the cryogenic cooling condition, tensile tests at different temperatures were carried out, which are used to study the changing trend of mechanical properties of TA15 alloy at low temperatures. Furthermore, through the machining experiments, the results of mechanical test analysis are verified, and the effectiveness of cutting TA15 alloy under cryogenic conditions is studied.

2.1 Tensile test

For the analysis of mechanical properties of TA15 at different temperatures, some scholars have carried out relevant research in a high-temperature environment [20, 22, 23]. However, there is no related study on the mechanical properties of TA15 at different temperatures in a low-temperature environment. To analyze the mechanical properties of TA15 at different temperatures, tensile tests were carried out. The chemical composition of the material used in the test is summarized in Table 1. Tensile specimens and geometrical dimensions are shown in Fig. 1.

The tensile tests were carried out at 25 °C, 0 °C, −50 °C, −100 °C, −150 °C, and −196 °C using MTS universal testing machine (CMT5000, USA) along the axial direction of the specimens under a strain rate of 10^{-3} s^{-1}, and each specimen was deformed until fracture.

The cryostat is filled with a certain amount of cryogenic gas or liquid, and the ambient temperature of the workpieces is controlled by the thermostat. The tensile tests platform is shown in Fig. 2.

2.2 Machining experiments

In order to verify the conclusions obtained by tensile test analysis, it is necessary to carry out TA15 cryogenic machining test verification.

A cylinder workpiece of TA15 material was machined having dimensions of 40 mm × φ30 mm in this experiment. The experiments were performed on a horizontal lathe manufactured by Dalian Machine Tool Group (CD6140A, China). Liquid nitrogen was provided by a liquid nitrogen tank (Tianhai DPL-175, China). A self-developed flow control device was applied to control the flow of liquid nitrogen. Coated tungsten carbide inserts DNMG 150,608-MM1125 supplied by Sandvik-Coromant® were used as cutting tool inserts. A self-developed LN_2 internal cooling turning tool was used in the experiments, the working clearance angle is 5° the rake angle is 7° and the nose radius is 0.8 mm. The diameter of the LN_2 injection microholes is 2 mm.

The schematic diagram and object picture of a self-developed LN_2 internal cooling turning tool are shown in Fig. 3. According to the research of Hong and Ding [24], applying LN_2 to the tool rake face and flank face simultaneously leads

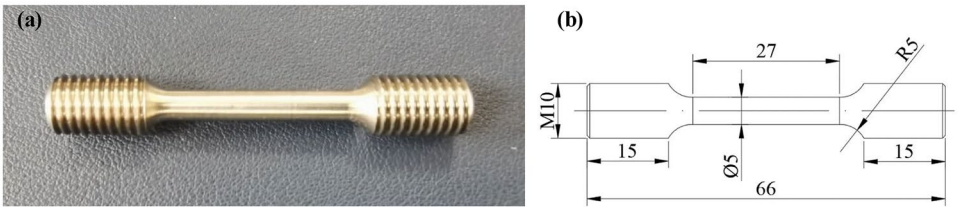

Fig. 1 Tensile specimens. (**a**) Object picture. (**b**) Geometrical dimension

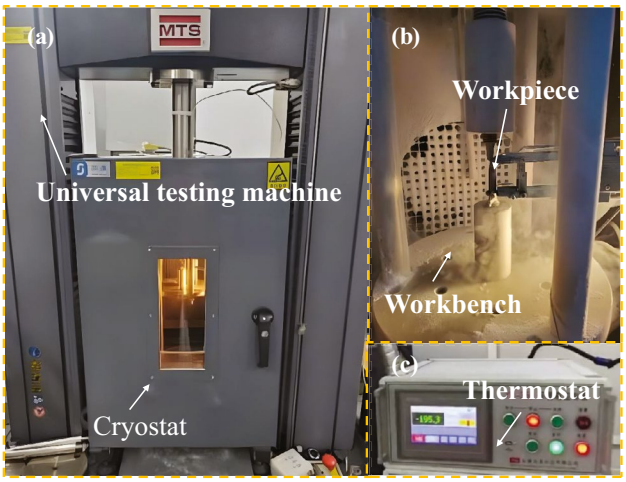

Fig. 2 Tensile test platform. (**a**) Universal testing machine. (**b**) Workbench. (**c**) Thermostat

to the most significant cooling effect. So, the internal cooling turning tool is designed to cool the rake face and flank face at the same time. Because LN_2 is easy to vapor, a heat insulation protective sleeve is provided in the main channel. To order to obtain a high cooling efficiency, the relationship between the microhole diameter and the jet distance should satisfy Eq.(1) [25].

$$S_p = \frac{1}{\sqrt{2C}}\sqrt{\frac{\rho_0}{\alpha\rho_l + (1-\alpha)\rho_g}}d_0 \quad (1)$$

where ρ_0 is the average initial density of microhole outlet cross section, ρ_l is the density of LN_2, ρ_g is the density of N_2, α is the volume fraction of LN_2, d_0 is the diameter of the microhole, S_p is the jet distance, and expansion coefficient $C = 0.114$ [26].

The experimental setup is shown in Fig. 4. The experiments were carried under three cooling conditions: dry, wet (cutting fluid), and cryogenic (liquid nitrogen internal cooling). The design of the experiment is shown in Table 2.

For the measurement equipment, the roughness of the machined surfaces was measured by the Taylor Hobson measurement system for the surface profile (Talysurf CLI200003191213, UK). The surface morphology and tool wear were observed by FEI scanning electron microscope (SEM) (Q45, USA).

The cutting fluid injection angle is 45°, and injection distance is 30 mm. According to the research of Tahmasebi et al. [27], it shows benefits for the cooling process for efficient cooling when the injection pressure is in the range of 0.2–0.4 MPa, so the LN_2 applied pressure is set to 0.4 MPa in the experiments of this paper. The ambient temperature is 20 °C, and the LN_2 temperature is −196 °C.

In the experiments, a cutting speed of 105 m/min and 130 m/min and a feed rate of 0.05 mm/rev and 0.14 mm/rev are adopted, respectively. Radial cutting depth is 0.2 mm, and feed length is 45 mm.

3 Results and discussion

3.1 Analysis of tensile test results

It can be seen from the tensile curve (Fig. 5) that with the decrease of temperature, the tensile specimens are still in the plastic fracture stage, and there is no plastic-brittle transition. However, the plasticity decreases, and the fracture elongation decreases when the temperature decrease. According to Fig. 6, with the decrease of temperature, the yield strength and tensile strength of the material increase, and the elongation of the cross-section also shows a downward trend, which indicates that the plasticity of TA15 decreases with the decrease of temperature.

3.2 Analysis of fracture morphology

The dimple size reflects the plastic deformation of the material before fracture. The larger the dimple size is, the better the plasticity is. As shown in Fig. 7, at 25 °C, the dimple size is larger, and the maximum is about 20 μm. With the decrease of temperature, the dimple size gradually decreases, indicating that the plasticity of TA15 decreases with the decrease of temperature, which confirms the analysis conclusion of the tensile curve in the previous.

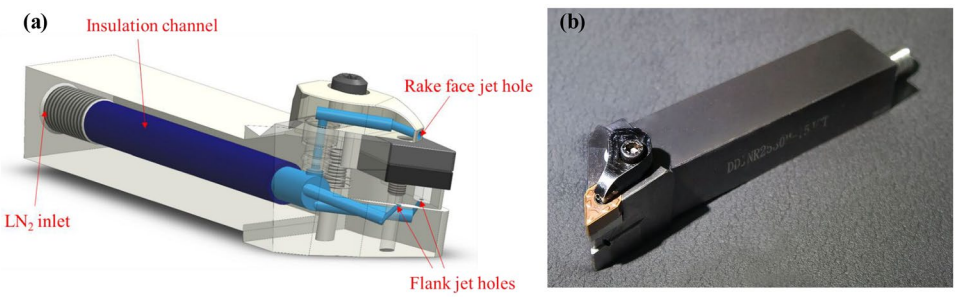

Fig. 3 LN_2 internal cooling turning tool. (**a**) Schematic diagram. (**b**) Object picture

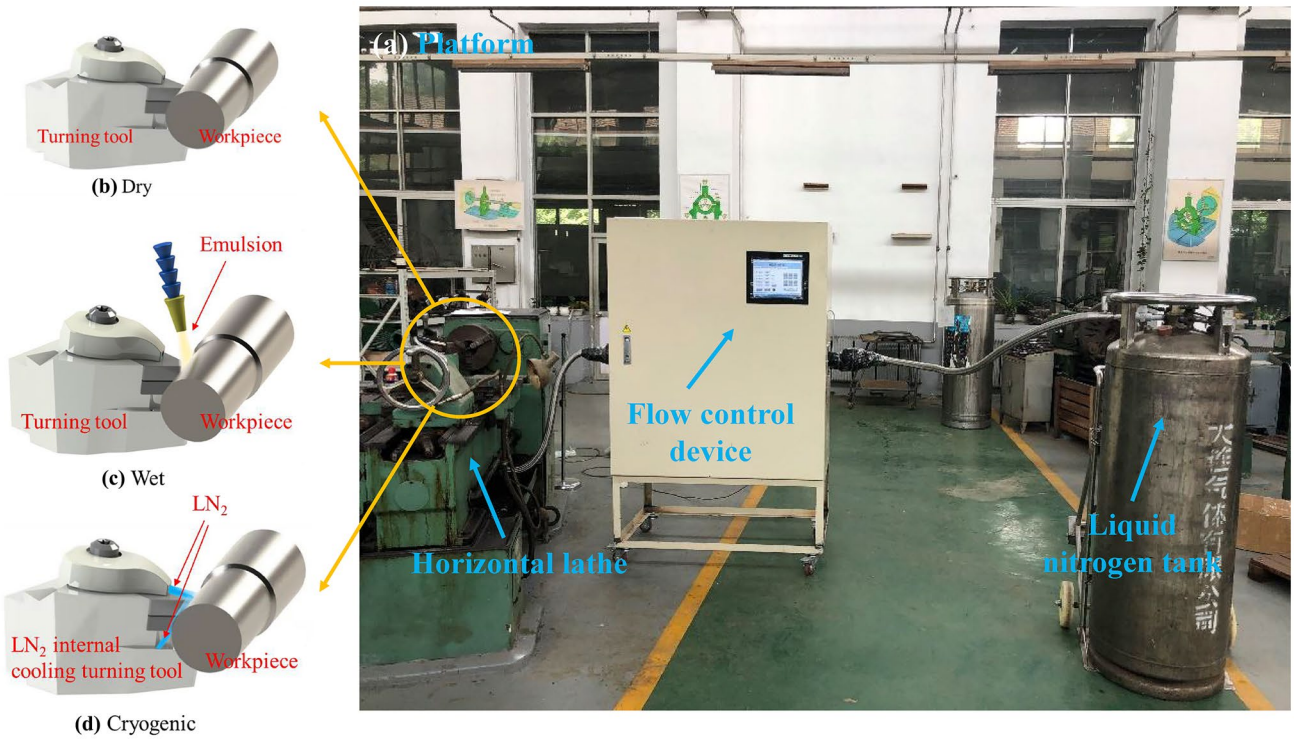

Fig. 4 Experimental setup for the experiments. (**a**) Platform. (**b**) Dry. (**c**) Wet. (**d**) Cryogenic

According to the fracture morphology at different ambient temperatures, it can be analyzed that the tensile strength of TA15 increases with the decrease of temperature, which leads to the improvement of the ability of the material to resist crack propagation. The relation between dislocation velocity V and temperature T can be expressed by Eq. (2) [28].

$$V = V_0\left(\frac{\tau}{\tau_0}\right)^n \exp\left(-\frac{\Delta F}{kT}\right)^{\frac{1}{n}} \tag{2}$$

Table 2 Design of experiment

No	Cutting speed (m/min)	Feed rate (mm/rev)	Cooling condition
1	105	0.05	Dry
2	105	0.14	Dry
3	130	0.05	Dry
4	130	0.14	Dry
5	105	0.05	Wet
6	105	0.14	Wet
7	130	0.05	Wet
8	130	0.14	Wet
9	105	0.05	Cryogenic
10	105	0.14	Cryogenic
11	130	0.05	Cryogenic
12	130	0.14	Cryogenic

where V_0 and τ_0 are constants of the material and ΔF is the activation energy for lattice resistance controlled glide, k is Boltzmann's constant, and T is the temperature. The exponent n is the dislocation velocity stress index.

It can be seen from Eq. (2) that when the temperature is below zero, the dislocation velocity decreases with the decrease of temperature. It can be inferred that at low-temperature conditions, the gap between atoms decreases, and the bonding force between atoms increases, which leads to the difficulty of dislocation slip. Thus, smaller dimples are formed.

The cavities formed during tensile at low temperature cannot grow into large dimples, and the fracture dimple morphology is small. The schematic diagram is shown in Fig. 8.

The better the plasticity of the material, the easier it is to produce the adhesion phenomenon in the machining process. Compared with normal temperature, the plasticity of the material under a low-temperature environment is reduced, and it is easier to be cut off, which can inhibit the production of adhesion phenomenon in the machining process. The conclusion analyzed by the tensile test will be verified by machining experiment results in the next section.

3.3 Surface roughness

This section discusses the machining surface roughness under different cooling conditions and different cutting

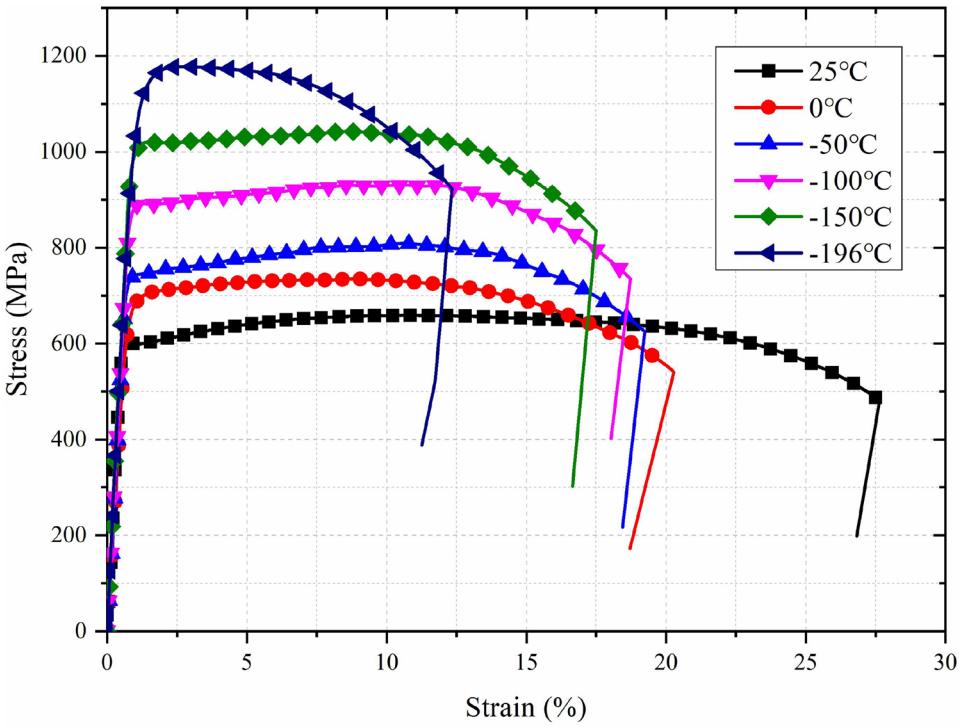

Fig. 5 Stress–strain curves of the specimens deformed at different temperatures

parameters. The surface roughness of workpieces is measured by Taylor Hobson measurement system.

In order to reduce the measurement error, three different positions of each sample were randomly selected, and the sampling length of each position is 4 mm. After the measurement, the comparison of the average values of surface roughness under different cooling conditions and different cutting parameters in the experiments is shown in Fig. 9.

Among the four groups of parameters, the roughness value of liquid nitrogen cooling is the lowest. Except that when the cutting speed v_c is 105 m/min and the feed rate f is 0.05 mm/rev, the roughness under the dry condition of the other three groups was greater than that of the other two cooling conditions. Especially when the feed rate is 0.14 mm/rev, the roughness under dry conditions is significantly greater than that of the other two groups. Compared with the maximum roughness, the roughness under cryogenic cooling condition decreased by 28% (v_c 105 m/min, f 0.05 mm/rev), 38% (v_c 105 m/min, f 0.14 mm/rev), 45% (v_c 130 m/min, f 0.05 mm/rev), and 32% (v_c 130 m/min, f 0.14 mm/rev), respectively.

In addition, under the same cooling conditions, the influence of cutting speed v_c on roughness is significantly smaller than the feed rate f. The larger the feed rate, the higher the roughness. When the feed rate is increased, the surface roughness will increase at the same time, and LN_2

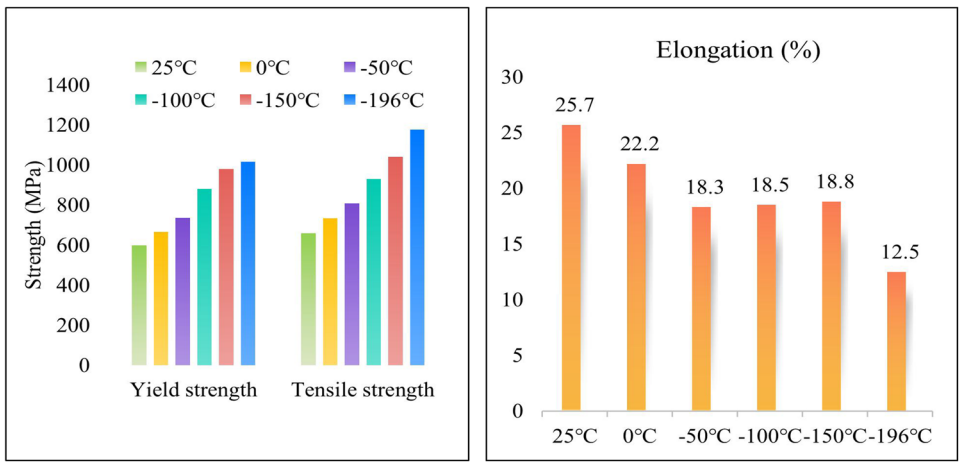

Fig. 6 Yield strength, tensile strength, and section elongation at different temperatures

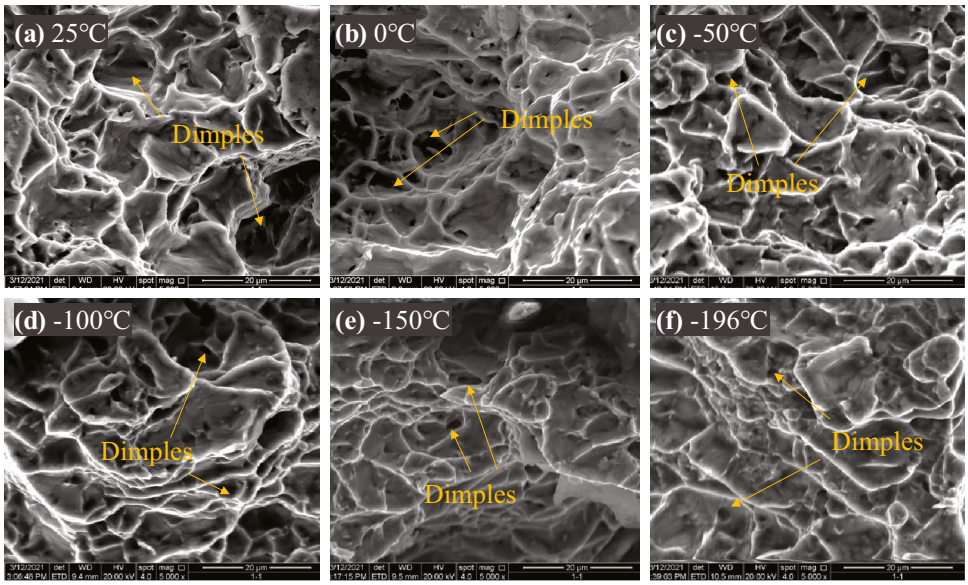

Fig. 7 SEM micrographs of tensile fracture surface at different temperatures. (**a**) 25 °C. (**b**) 0 °C. (**c**) −50 °C. (**d**) −100 °C. (**e**) −150 °C. (**f**) −196 °C

internal cooling is no exception. This is also consistent with the findings of Bordin et al. [17]. It indicates that although cryogenic cooling effectively reduces the roughness, it cannot offset the impact of increasing the feed rate. In order to improve the roughness of the machined surface, it is necessary to reduce the feed rate while using cryogenic cooling.

Furthermore, it is necessary to observe the machined surface morphology to analyze the causes of roughness differences.

3.4 Surface morphology

As shown in Fig. 10, there are many defects on the dry cutting surface. Under different cutting parameters, there are serious adhesion phenomena under dry conditions, accompanied by side flow and thick feed marks. It indicates that under dry cutting conditions, cutting TA15 generates a large amount of cutting heat, and TA15 titanium alloy will show better plasticity under high temperatures [20]. As a result, it is more difficult to remove the material in the cutting process, resulting in a lot of surface defects.

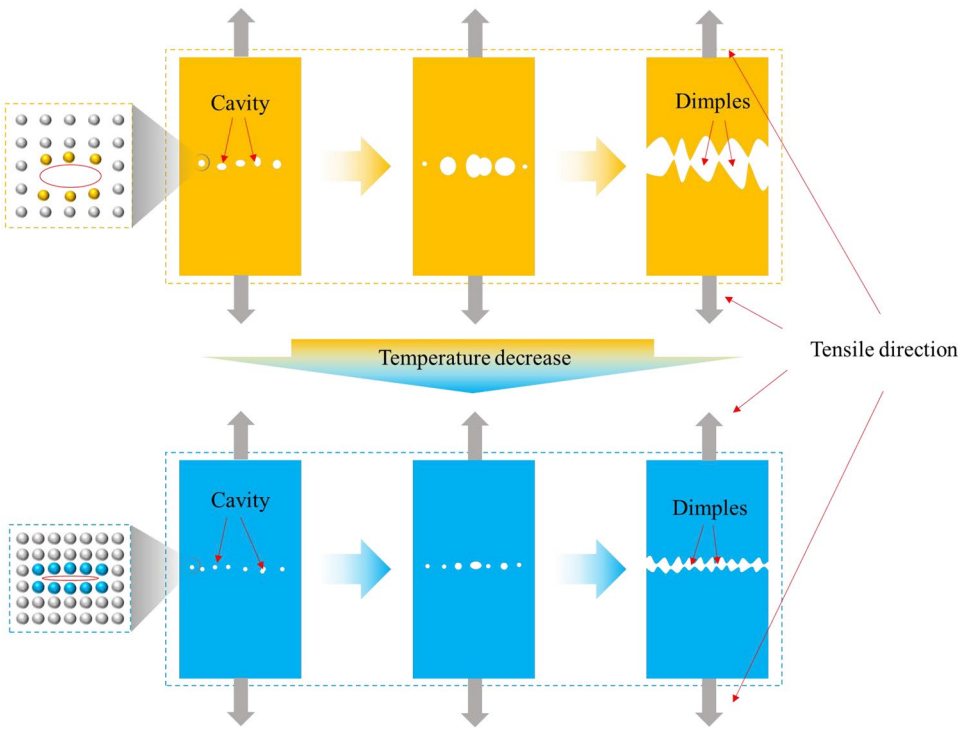

Fig. 8 Comparison of dimples formation at high and low temperatures

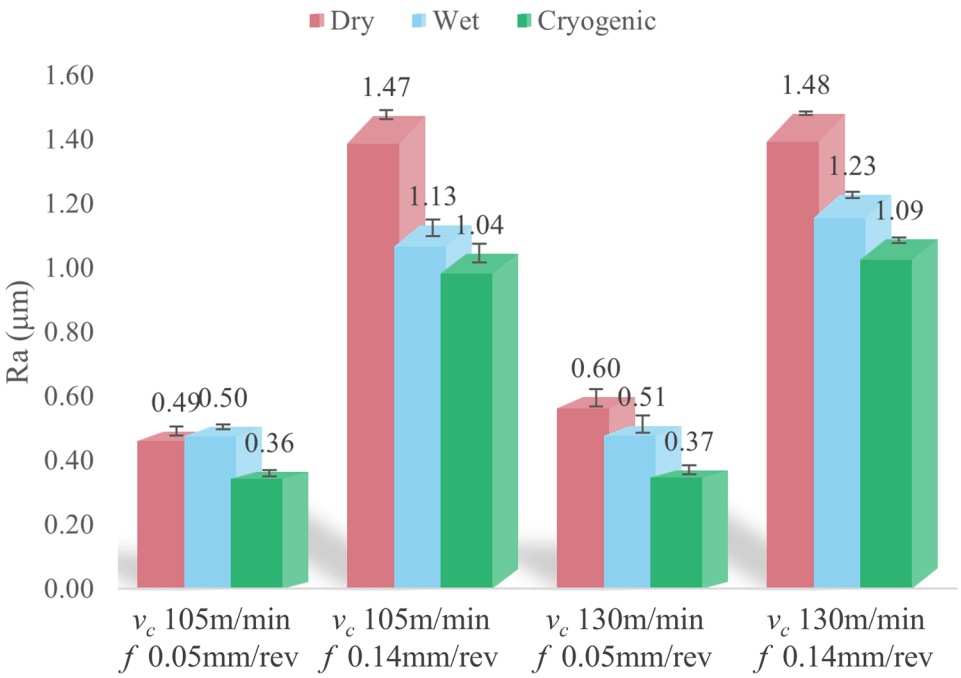

Fig. 9 Comparison of the surface roughness under different cooling conditions and different cutting parameters in the experiments

Under wet conditions, the surface quality is better than that of dry cutting. However, there are still adhesion, side flow, and thick feed marks. Especially when the cutting speed v_c is 105 mm/min and the feed f is 0.14 mm/rev, the groove phenomenon is obvious, which may be caused by built-up edge. According to the analysis of the surface morphology, it shows that although the cutting fluid has the effect of cooling and lubrication, it is not enough to inhibit the formation of adhesion and other defects on the machined surface of TA15.

Compared with the former two cooling methods, there is only a small amount of adhesion phenomenon on the machined surface by cryogenic cooling under various parameters. It indicates that under low-temperature conditions, the material is easier to fracture due to the decrease of plasticity. Therefore, the generation of feed marks, side flow, and adhesion phenomenon is inhibited, and the surface quality is improved. At the same time, the conclusion analyzed by the tensile test is also confirmed.

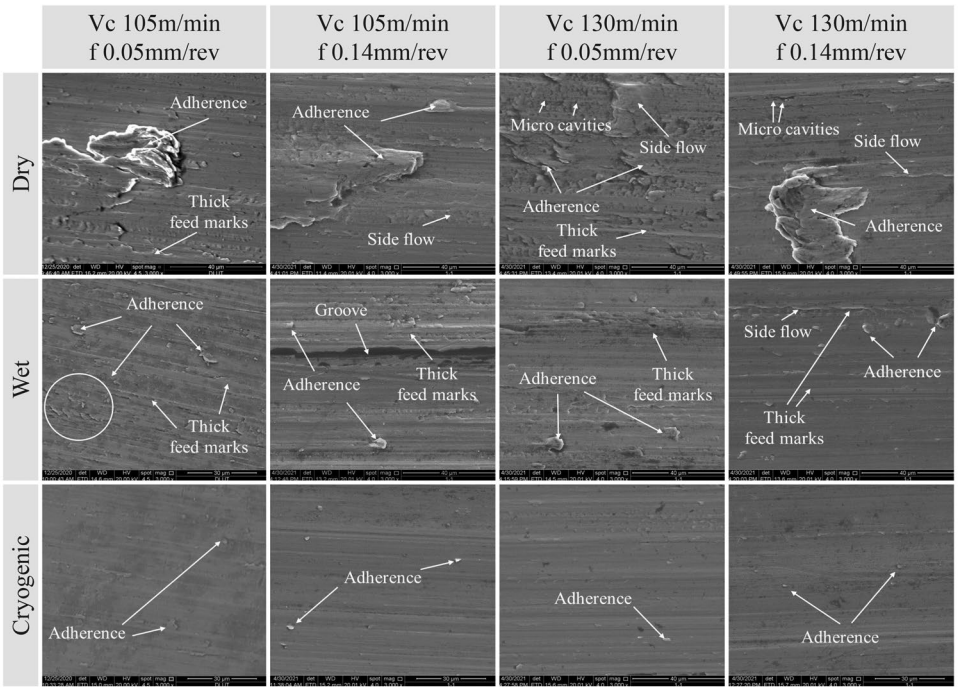

Fig. 10 SEM micrographs (3000×) of machined surface under different cooling conditions and different cutting parameters in the experiments

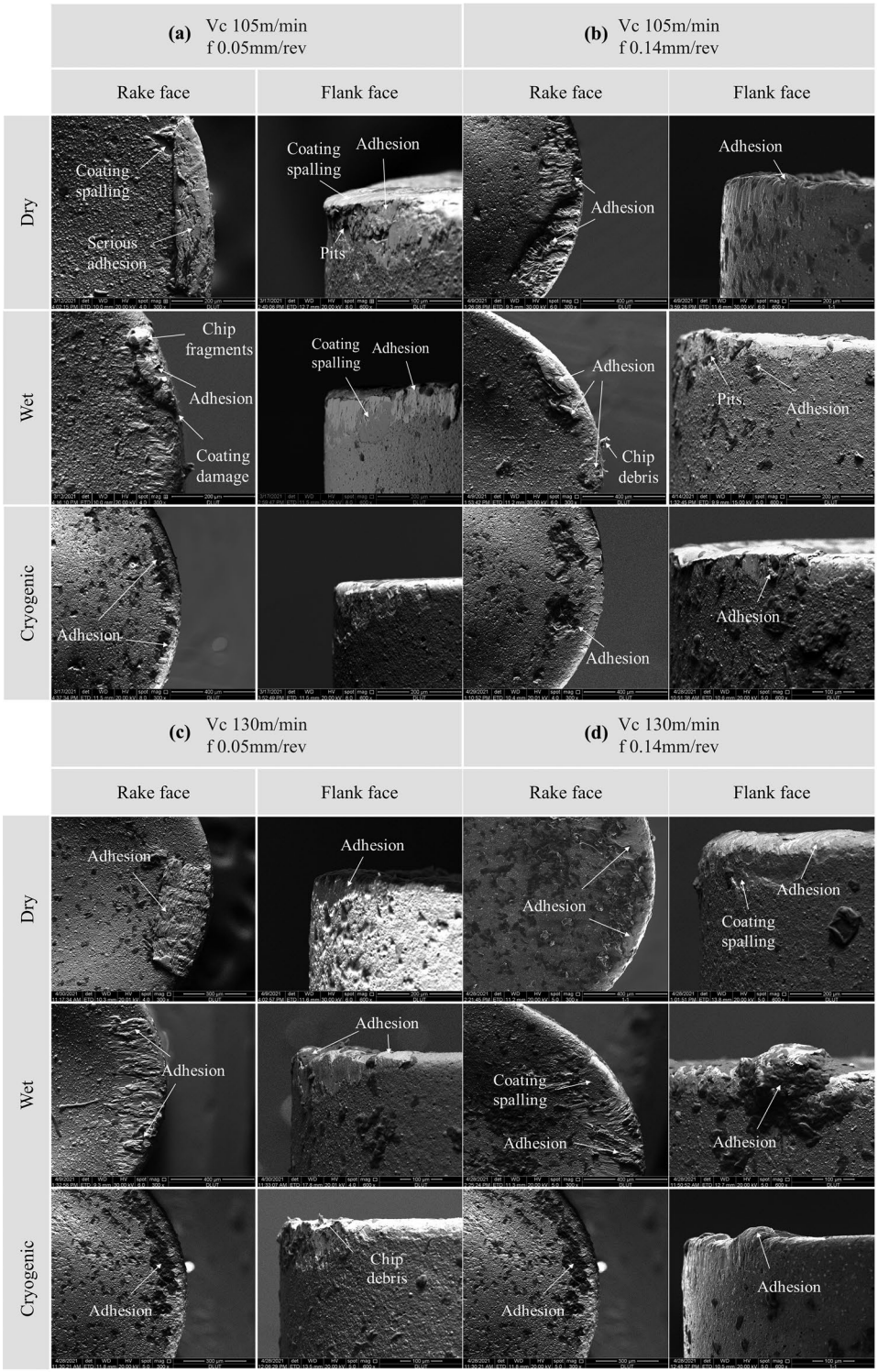

Fig. 11 Tool inserts SEM micrographs of rake (300×) and flank face (600×) under different cooling conditions and different cutting parameters in the experiments. (**a**) v_c 105 m/min, f 0.05 mm/rev. (**b**) v_c 105 m/min, f 0.14 mm/rev. (**c**) v_c 130 m/min, f 0.05 mm/rev. (**d**) v_c 130 m/min, f 0.14 mm/rev

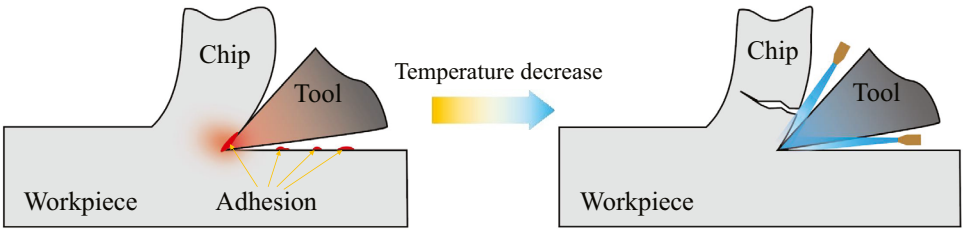

Fig. 12 Diagram illustrating the effects of lowering the temperature on the machining

3.5 Tool wear

In addition to the quality of the machined surface, the tool wear characteristics of the tool surface also reflect the characteristics of the material removal process.

Figure 11 shows the SEM images of tool wear under different cutting parameters and cooling conditions. As shown in Fig. 11, under the condition of dry cutting, because dry cutting has no cooling effect, the rake and flank face of the cutting tool inserts have different degrees of adhesion, especially on the rake face of the tool inserts. Under the condition of dry cutting, the rake face has large block adhesion, and the flank face also has a certain degree of adhesion.

Under the wet cooling condition, the adhesion phenomenon is not obvious as that of dry cutting. However, there is still a large area of adhesion on the rake face. On the flank, although the adhesion phenomenon is not as serious as that of the rake face, there are still some serious adhesion phenomena under some parameters, such as v_c 130 m/min and f 0.14 mm/rev; a large block of adhesion occurs in the flank face. Although the cutting fluid has some cooling and lubrication effect, the cooling efficiency is insufficient when cutting TA15.

Compared with the other two cooling conditions, under the cryogenic cooling condition, the tool adhesion phenomenon is the least due to the high cooling efficiency. And there is only a small amount of adhesion phenomenon on the rake and flank face. This phenomenon is also consistent with the law of machined surface quality in the former parts of this paper.

In the process of machining, when the cooling efficiency is insufficient, with the high temperature generated during machining, the strength of the material decreases and the plasticity increases, resulting in the phenomenon of machined surface adhesion and tool adhesion. When the temperature drops, the plasticity and ductility of the material diminishes, which is not only conducive to chip breaking, but also aids in the reduction of adhesion, as illustrated in Fig. 12.

As shown in the studies of Sects. 3.1 and 3.2, the plasticity and ductility of TA15 is reduced under the cryogenic conditions and thus reduces the generation of adhesion during machining. The machining results in Sects. 3.4 and 3.5 also verify the research results in Sects. 3.1 and 3.2.

4 Conclusion

In this paper, the feasibility of TA15 machining under cryogenic cooling conditions was studied. The change of mechanical properties of the material at low temperature was analyzed by mechanical experiments, and the mechanism of the change was analyzed. Through the comparative cutting experiments of TA15 under different cooling conditions, the experimental results are analyzed from the aspects of surface morphology, surface roughness, and tool wear.

The main findings of this investigation can be summarized as follows:

1. Low-temperature environment has a significant impact on the machinability of TA15 titanium alloy. The plasticity of TA15 titanium alloy decreases at low temperatures. It helps to reduce the generation of adhesion, and it is easier to fracture during the machining process.
2. Compare with the dry and wet cooling conditions, machining TA15 under cryogenic cooling conditions can effectively reduce the defects such as feed marks, side flow, and adhesion on the machined surface and improve the surface quality and surface roughness.
3. The adhesion wear of the cutting tool inserts is effectively inhibited under the internal cryogenic cooling conditions when machining TA15. Moreover, the tool life is also improved.

Funding This research is funded in part by National Key R&D Program of China (2019YFB2005400), Changjiang Scholar Program of the Chinese Ministry of Education (T2017030), and Top and Leading Talents of Dalian (2018RD05).

Declarations

Ethical approval The authors oblige the rules regarding the ethic in publication.

Consent to participate All authors consent to participate.

Consent for publication All authors consent to publish.

Competing interests The authors declare no competing interests.

References

1. Ezugwu EO (2005) Key improvements in the machining of difficult-to-cut aerospace superalloys. Int J Mach Tools Manuf 45:1353–1367. https://doi.org/10.1016/j.ijmachtools.2005.02.003
2. Gupta MK, Sood PK, Sharma VS (2016) Optimization of machining parameters and cutting fluids during nano-fluid based minimum quantity lubrication turning of titanium alloy by using evolutionary techniques. J Clean Prod 135:1276–1288. https://doi.org/10.1016/j.jclepro.2016.06.184
3. Gupta MK, Song Q, Liu Z, Sarikaya M, Mia M, Jamil M, Singla AK, Bansal A, Pimenov DY, Kuntoğlu M (2021) Tribological performance based machinability investigations in cryogenic cooling assisted turning of α-β titanium Alloy. Tribol Int 160:107032. https://doi.org/10.1016/j.triboint.2021.107032
4. Shokrani A, Dhokia V, Newman ST (2012) Environmentally conscious machining of difficult-to-machine materials with regard to cutting fluids. Int J Mach Tools Manuf 57:83–101. https://doi.org/10.1016/j.ijmachtools.2012.02.002
5. Singh R, Dureja J S, Dogra M, Kumar Gupta M, Jamil M, Mia M (2020) Evaluating the sustainability pillars of energy and environment considering carbon emissions under machining ofTi-3Al-2.5 V. Sustain Ener Technol Assess 42:100806. https://doi.org/10.1016/j.seta.2020.100806
6. Tahri C, Lequien P, Outeiro JC, Poulachon G (2017) CFD Simulation and optimize of LN2 flow inside channels used for cryogenic machining: application to milling of titanium alloy Ti-6Al-4V. Procedia CIRP 58:584–589. https://doi.org/10.1016/j.procir.2017.03.230
7. Tu L, Chen J, An Q, Ming W, Xu J, Chen M, Lin L, Yang Z (2021) Machinability improvement of compacted graphite irons in milling process with supercritical CO2-based MQL. J Manuf Process 68:154–168. https://doi.org/10.1016/j.jmapro.2021.05.044
8. Jawahir IS, Attia H, Biermann D, Duflou J, Klocke F, Meyer D, Newman ST, Pusavec F, Putz M, Rech J (2016) Cryogenic manufacturing processes. CIRP Ann Manuf Technol. https://doi.org/10.1016/j.cirp.2016.06.007
9. Khanna N, Agrawal C, Gupta MK, Song Q (2020) Tool wear and hole quality evaluation in cryogenic drilling of Inconel 718 superalloy. Tribol Int 143:106084. https://doi.org/10.1016/j.triboint.2019.106084
10. Jayal AD, Badurdeen F, Dillon Jr OW, Jawahir IS (2010) Sustainable manufacturing: modeling and optimization challenges at the product, process and system levels. CIRP J Manuf Sci Technol 2:144–152. https://doi.org/10.1016/j.cirpj.2010.03.006
11. Biek M, Dumont F, Courbon C, Puavec F, Kopa J (2012) Cryogenic machining as an alternative turning process of normalized and hardened AISI 52100 bearing steel. J Mater Process Tech 212:2609–2618. https://doi.org/10.1016/j.jmatprotec.2012.07.022
12. Yang S, Puleo DA, Dillon OW, Jawahir IS (2011) Surface layer modifications in Co-Cr-Mo biomedical alloy from cryogenic burnishing. Proc Eng 19:383–388. https://doi.org/10.1016/j.proeng.2011.11.129
13. Pu Z, Outeiro JC, Batista AC, Dillon OW Jr, Puleo DA, Jawahir IS (2012) Enhanced surface integrity of AZ31B Mg alloy by cryogenic machining towards improved functional performance of machined components. Int J Mach Tools Manuf 56:17–27. https://doi.org/10.1016/j.ijmachtools.2011.12.006
14. Schoop J, Ambrosy F, Zanger F, Schulze V, Jawahir IS, Balk TJ (2015) Increased surface integrity in porous tungsten from cryogenic machining with cermet cutting tool. Mater Manuf Processes. https://doi.org/10.1080/10426914.2015.1048467
15. Xia T, Kaynak Y, Arvin C, Jawahir IS (2015) Cryogenic cooling-induced process performance and surface integrity in drilling CFRP composite material. Int J Adv Manufact Technol. https://doi.org/10.1007/s00170-015-7284-y
16. Gan Y, Wang Y, Liu K, Han L, Luo Q, Liu H (2020) A novel and effective method for cryogenic milling of polytetrafluoroethylene. Int J Adv Manufact Technol 112:969–976. https://doi.org/10.1007/s00170-020-06332-4
17. Bordin A, Sartori S, Bruschi S, Ghiotti A (2017) Experimental investigation on the feasibility of dry and cryogenic machining as sustainable strategies when turning Ti6Al4V produced by additive manufacturing. J Clean Prod 142:4142–4151. https://doi.org/10.1016/j.jclepro.2016.09.209
18. Shokrani A, Dhokia V, Newman ST (2016) Investigation of the effects of cryogenic machining on surface integrity in CNC end milling of Ti-6Al-4V titanium alloy. J Manuf Process 21:172–179. https://doi.org/10.1016/j.jmapro.2015.12.002
19. Bermingham MJ, Kirsch J, Sun S, Palanisamy S, Dargusch MS (2011) New observations on tool life, cutting forces and chip morphology in cryogenic machining Ti-6Al-4V. Int J Mach Tools Manuf 51:500–511. https://doi.org/10.1016/j.ijmachtools.2011.02.009
20. Hao F, Xiao J, Feng Y, Wang Y, Tan C (2020) Tensile deformation behavior of a near-α titanium alloy Ti-6Al-2Zr-1Mo-1V under a wide temperature range. J Market Res. https://doi.org/10.1016/j.jmrt.2020.01.016
21. Chen R, Tan C, You Z, Li Z, Zhang S, Nie Z, Yu X, Zhao X (2019) Effect of α phase on high-strain rate deformation behavior of laser melting deposited Ti-6.5Al-1Mo-1V-2Zr titanium alloy. Mater Sci Eng A. https://doi.org/10.1016/j.msea.2019.01.060
22. Gao P, Zhan M, Fan X, Lei Z, Cai Y (2017) Hot deformation behavior and microstructure evolution of TA15 titanium alloy with nonuniform microstructure. Mater Sci Eng A 689:243–251. https://doi.org/10.1016/j.msea.2017.02.054
23. Liu G, Wang K, He B, Huang M, Yuan S (2015) Mechanism of saturated flow stress during hot tensile deformation of a TA15 Ti alloy. Mater Des 86:146–151. https://doi.org/10.1016/j.matdes.2015.07.100
24. Hong SY, Ding Y (2001) Cooling approaches and cutting temperatures in cryogenic machining of Ti-6Al-4V. Int J Mach Tools Manuf 41:1417–1437. https://doi.org/10.1016/S0890-6955(01)00026-8
25. Gan Y, Wang Y, Liu K, Wang S, Yu Q, Che C, Liu H (2021) The development and experimental research of a cryogenic internal cooling turning tool. J Clean Prod. https://doi.org/10.1016/j.jclepro.2021.128787
26. Albertson ML, Dai YB, Jensen RA, Rouse H (1950) Diffusion of submerged jets. Transactions ASCE 115:639–664. https://doi.org/10.1061/TACEAT.0006302
27. Tahmasebi E, Albertelli P, Lucchini T, Monno M, Mussi V (2019) CFD and experimental analysis of the coolant flow in cryogenic milling. Int J Mach Tools Manuf 140:20–33. https://doi.org/10.1016/j.ijmachtools.2019.02.003
28. Ashby MF, Embury JD (1985) The influence of dislocation density on the ductile-brittle transition in BCC metals. Scr Metall 19:557–562. https://doi.org/10.1016/0036-9748(85)90134-6